Manuscript published in
Multiphase Science and Technology, 2008, Vol. 20. Issue 3-4, pp. 323-354.

NUMERICAL SCHEME OF THE WAHA CODE

I. Tiselj, A. Horvat, J. Gale
"Jožef Stefan" Institute
1000 Ljubljana, Slovenia

Abstract

This paper describes the numerical scheme used in the WAHA code that was developed within the WAHALoads project for simulations of fast transients in 1D piping systems. Two-fluid model equations are solved with an operator splitting procedure. A second-order accurate non-conservative characteristic upwind scheme is used to solve the hyperbolic part of the equations with the non-relaxation source terms, while the relaxation source terms are treated in the second step of the operator splitting procedure. The water-vapour properties are calculated with a newly developed set of subroutines that use pre-tabulated water properties. Special models that were developed for the treatment of the abrupt area-changes and branches in the piping systems are described. Various test cases, which were used to test the accuracy of the basic numerical scheme and the accompanying numerical models, are described together with typical results of the simulations.

1. Introduction

Among the eleven contractors of the WAHALoads project, three of them (UCL - Catholic University of Louvain, CEA-Grenoble and "Jozef Stefan" Institute) were developing a computer code named WAHA (Tiselj et. al. 2004) for prediction of 1D two-phase flows during water hammer events and shock wave propagation in pipes and open networks. The primary objective of this code is an accurate prediction of hydrodynamic loads on pipes during the fast transients. The physical models and the results of several fast transient simulations are given in the paper by Gale et. al. (2006), while the present paper describes the numerical scheme used in the WAHA code together with the cases that were used to test accuracy and robustness of the applied numerical methods. Larger number of works has been published in the past few years in the field of the numerical solutions of the hyperbolic two-fluid models for two-phase flows (e.g. Toumi and Kumbaro, 1996, Bereux, 1996, Burman and Sainsaulieu, 1995, Gallouet and Massela, 1996, Karni, 1996, Tiselj and Petelin, 1997, Saurel and Abgrall, 1999, Faucher et al., 2000, Ghidaglia et al., 2001, Guinot, 2001, Evje and Fjelde, 2002, Paillere et. al. 2003, Evje and Flatten, 2003). Most of these works are based on the evaluation of the characteristic velocities in the two-fluid models. They represent an extension of the numerical schemes used in aerodynamics to the field of two-fluid models of two-phase flows. In comparison to the so-called donor-based numerical schemes used in the system codes for the thermal-hydraulic analyses of the piping systems in nuclear power plants (RELAP - Carlson et.al., 1990, CATHARE - Bestion, 1990, TRAC - Spore et al., 1981), the characteristic-upwind schemes offer better control of the numerical uncertainties and the second-order accuracy of solutions. In general, the advantages of the characteristic-upwind schemes are not

solely sufficient to initiate the upgrade of the system codes with the improved numerical schemes. Namely, the main source of the inaccuracy in the system codes does not stem from the numerical scheme but rather from the incorporated physical models. Nevertheless, we estimated the advantages of the characteristic-upwind schemes as sufficient to justify their application in the new codes. Thus, the WAHA code was built on the characteristic-upwind numerical scheme.

While most of the research in the field of the characteristic-upwind schemes for the two-fluid models was focused on the solution of the hyperbolic part of the two-fluid model, only a small part of attention was focused on the source terms. In the computer code like WAHA, which attempts to cover rather wide spectra of the transients in the piping systems, integration of the source terms turned out to be a more difficult part of the task. Non-relaxation source terms describing exchange of mass, momentum and energy between the fluid and the environment are integrated with the same characteristic upwind numerical scheme as convective terms. Relaxation source terms describing internal exchange between the liquid and the gas phase are often stiff (Pember, 1993). They are integrated in a separate sub-step of the operator splitting method without upwinding.

The section 2 of the present paper describes the operator splitting approach used in WAHA code. The section 3 reviews the non-conservative characteristic-upwind numerical scheme used to integrate the convective part of the equations together with the non-relaxation source terms. Various examples are added to demonstrate the accuracy of the solutions. The integration of the relaxation source terms is the second sub-step of the operator splitting procedure and is described in the section 4. The section 5 reviews the models of the single-to-two-phase and the two-phase-to-single-phase flow transition, the section 6 describes calculation of the water-vapour properties, and the section 7 presents special models used in WAHA code to describe an abrupt area change and a branch in the piping systems. The last section lists the main conclusions and possible further modifications of the numerical procedures.

2. Operator splitting

The system of WAHA equations can be written in the following form:

$$\mathbf{A}\frac{\partial \vec{\psi}}{\partial t} + \mathbf{B}\frac{\partial \vec{\psi}}{\partial x} = \vec{S} \quad , \tag{1}$$

where $\vec{\psi}$ represents the vector of independent variables $\vec{\psi} = (p, \alpha, v_f, v_g, u_f, u_g)$, **A** and **B** are matrices of the system, and $\vec{S}$ is a vector with non-differential terms in the equations. The derivation of matrices **A** and **B** and vector $\vec{S}$ can be found in the WAHA code manual (Tiselj et. al., 2004) and in Gale et al. (2006). The numerical scheme of the WAHA code is based on non-conservative variables. Reasons that led to the choice of the non-conservative variables and consequences of such approach are analyzed later in the present paper.

The source term vector $\vec{S}$ in Equation (1) is further split into two parts:

$$\vec{S} = \vec{S}_{N-R} + \vec{S}_R \, . \tag{2}$$

The first part of the source term are "non-relaxation" sources $\vec{S}_{N-R}$, which contain wall friction, volumetric forces (gravity) and sources due to a variable pipe cross-section. The non-

relaxation source terms are closely related with convection terms and are treated together with the convection terms in the WAHA code using the method of Glaister (1985).

The second part of the source term contains relaxation sources $\vec{S}_R$, which tend to establish thermal and mechanical equilibrium between both phases, i.e., they are responsible for the inter-phase heat, mass, and momentum transfer. The relaxation sources are often stiff, i.e. their characteristic times are much shorter than the characteristic times of other phenomena in two-phase flow, even shorter than the characteristic times of the acoustic waves.

Stiffness of the relaxation sources is the reason for the use of the operator splitting in the numerical scheme of the WAHA code. Splitting means that the convection terms with the non-relaxation sources $\vec{S}_{N-R}$ in Equation (1) are treated separately from the relaxation sources $\vec{S}_R$. A single time step includes the following two sub-steps (superscripts $n, n+1$ denote time levels, * denotes intermediate time level and subscript *j* denotes spatial position):
1) The convection terms and the non-relaxation sources:

$$\vec{\psi}_j^{*} = \vec{\psi}_j^{n} - \Delta t \left(\left(\mathbf{A}^{-1} \vec{S}_{N-R} \right) + \left(\mathbf{A}^{-1} \mathbf{B} \right) \frac{\partial \vec{\psi}^{n}}{\partial x} \right)_j . \tag{3}$$

2) Intermediate values in the vector $\vec{\psi}_j^{*}$ are initial conditions for integration of the relaxation sources:

$$\vec{\psi}_j^{n+1} = \vec{\psi}_j^{*} + \int_{t^*}^{t^*+\Delta t} \mathbf{A}^{-1} \left(\vec{\psi}_j^{*} \right) \vec{S}_R \left(\vec{\psi}_j^{*} \right) dt . \tag{4}$$

The operator splitting given by Eqs. (3) and (4) is formally first-order accurate. However, the numerical tests have shown, that despite the formally lower order of accuracy, the results are practically the same as with the second-order accurate Strang splitting (LeVeque, 1992), which was coded in one of the earlier versions of the code. A detailed scheme for each sub-step of the operator splitting is given in the next sub-sections.

The operator splitting as shown in Eqs. (3)-(4) is a very simple and "easy-to-use" tool. However, it is also a source of a specific non-accuracy, which was discussed by Burman and Sainsaulieu (1995), Bereux (1996), and Tiselj and Horvat (2002). The papers of Burman and Sainsaulieu (1995), and Bereux (1996) are from the area of particle-gas two-phase flow during rocket fuel combustion. They discuss a problem of solving a system of hyperbolic equations of the same form as Eq. (1) written as:

$$\frac{\partial \varphi}{\partial t} + C \frac{\partial \varphi}{\partial x} = \frac{\varphi - \varphi^{*}}{\varepsilon} \tag{5}$$

where superscript * denotes the equilibrium (thermal or mechanical) value and ε denotes the characteristic time of relaxation. The relaxation time is a time period in which the relaxation quantity φ approaches to its equilibrium value φ^{*}. Numerical solution of the Eq. (5), obtained with operator splitting method, converges toward the solution of the differential Equation (5) as $\Delta x \to 0,\ \Delta t \to 0$ and when the condition $\Delta t / \varepsilon$ is fulfilled. The last condition is often not respected in the two-fluid codes. It is clear that the problems appear for small values of the relaxation time ε.

Up to four types of non-equilibrium (relaxation variables) can be present in the two-phase water system; each of them has different characteristic relaxation time:

1) Different phasic pressures: exact relaxation times unknown - known to be very short.
2) Vapor temperature not in saturation - relaxation times short in most of the flow regimes, but not always negligible.
3) Liquid temperature not in equilibrium - relaxation time not negligible.
4) Mechanical non-equilibrium: different phase velocities - relaxation time not negligible.

The six-equation model of the WAHA code describes the non-equilibrium no. 2, 3 and 4. The five-equation model would be sufficient to describe the non-equilibrium no. 3 and 4, the seven-equation model of Saurel and Abgrall (1999) can describe all four types of non-equilibrium, whereas the simplest three-equation homogeneous-equilibrium model (HEM) cannot describe any kind of non-equilibrium. From the physical point of view, more equations describe the system more accurately. However, each type of non-equilibrium combined with the operator splitting method causes numerical error, which behaves like numerical diffusion when the relaxation time is very short. This is demonstrated in the two-phase shock tube problem presented in the section 4 of the present paper.

Because of the numerical non-accuracy of the operator splitting method, it is better to use two-fluid model with less equations for very short relaxation times. If all relaxation times are very short, the three-equation HEM model is the optimal approach. On the other hand, relaxation times must be estimated from the existing physical models for different types of non-equilibrium. Short and long relaxation times for the non-equilibrium types no. 2, 3, and 4 are encountered in two-phase flows of water. Therefore, it was decided to use six-equation two-fluid model in the WAHA code.

User of the WAHA code should be aware of the deficiency of the applied operator splitting method, which is seen as an additional numerical diffusion when very short relaxation times appear in the equations. With a special transformation of the equations and with appropriate numerical schemes described by Burman and Sainsaulieu (1995), and Bereux (1996), this deficiency of the operator splitting method can be avoided. However, due to their complexity, and due to the fact that the performance of these models would be questionable for non-stiff relaxation terms, these approaches are not applied in the WAHA code.

3. Discretisation of the convective terms with the non-relaxation source terms

Equation (1) multiplied by $\mathbf{A}^{-1}$ from the left gives

$$\frac{\partial \vec{\psi}}{\partial t} + \mathbf{C}\frac{\partial \vec{\psi}}{\partial x} = \mathbf{A}^{-1} \cdot \vec{S}_{N-R} \ , \tag{6}$$

where $\mathbf{C} = \mathbf{A}^{-1}\mathbf{B}$ is the Jacobian matrix, which can be diagonalised as

$$\mathbf{C} = \mathbf{L} \cdot \mathbf{\Lambda} \cdot \mathbf{L}^{-1} \ . \tag{7}$$

The diagonal matrix $\mathbf{\Lambda}$ is the matrix of eigenvalues and $\mathbf{L}$ is the matrix of eigenvectors of the matrix $\mathbf{C}$. Eigenvalues, eigenvectors, and inverse matrix of eigenvectors are explicitly calculated between the grid points in the WAHA code. In order to use the numerical scheme described in this report, the system of equations (6) must be hyperbolic. This is not always the

case for six-equation two-fluid models. However, as mentioned in the paper by Gale et. al (2006), the hyperbolicity of the WAHA code equations is ensured with appropriate form of the additional differential terms for virtual mass and/or interfacial pressure. The calculation in the WAHA code is interrupted if complex eigenvalues are found and the equations become non-hyperbolic. However, such cases were never recorded in simulations of the physical phenomena.

Diagonalization of the Jacobian matrix (7) is performed numerically for the reduced matrix **C** of dimension 4x4, while the remaining two eigenvalues and eigenvectors are calculated analytically. The approximate analytical approach in computation of the eigenvalues was avoided in order to make the code more general and to allow easier introduction of the correlations that might contain derivatives, which would modify the eigen-structure of the equations. A specific problem of the six-equation two-fluid models of two-phase flow is degeneration of a pair of eigenvectors when relative inter-phase velocity is zero. In this case only five linearly independent eigenvectors exist. The problem remains solvable, if a small artificial relative velocity is maintained; the value $|v_r| = 10^{-7}\ m/s$ is used in the WAHA code.

The non-relaxation source term $\mathbf{A}^{-1}\vec{S}_{N-R}$ in Eq. (6) is written in two parts as

$$\mathbf{A}^{-1}\vec{S}_{N-R} = -\vec{R}_A \frac{dA(x)}{dx} - \vec{R}_F \,. \tag{8}$$

The first part with the vector $\vec{R}_A$ contains source terms due to the variable pipe cross-section with derivatives of the pipe cross-section, and the second part $\vec{R}_F$ contains wall friction and volumetric forces withno derivatives. Using Eqs. (7) and (8), Eq. (6) is written as:

$$\frac{\partial \vec{\psi}}{\partial t} + \mathbf{L}\cdot\mathbf{\Lambda}\cdot\mathbf{L}^{-1}\frac{\partial \vec{\psi}}{\partial x} + \vec{R}_A\frac{\partial A}{\partial x} + \vec{R}_F = 0 \,. \tag{9}$$

The total derivative of cross-section *A* can be replaced with a partial derivative, as *A* is only a function of *x*. This equation is multiplied by $\mathbf{L}^{-1}$ from the left and modified with identities $\mathbf{\Lambda}\cdot\mathbf{\Lambda}^{-1} = \mathbf{I}$ and $\frac{\partial x}{\partial x} = 1$ to:

$$\mathbf{L}^{-1}\frac{\partial \vec{\psi}}{\partial t} + \mathbf{\Lambda}\cdot\mathbf{L}^{-1}\frac{\partial \vec{\psi}}{\partial x} + \mathbf{\Lambda}\cdot\mathbf{\Lambda}^{-1}\cdot\mathbf{L}^{-1}\vec{R}_A\frac{\partial A}{\partial x} + \mathbf{\Lambda}\cdot\mathbf{\Lambda}^{-1}\cdot\mathbf{L}^{-1}\vec{R}_F\frac{\partial x}{\partial x} = 0 \,. \tag{10}$$

Modified characteristic variables (Glaister, 1985) are then introduced in Eq. (10) as

$$\delta\vec{\xi} = \mathbf{L}^{-1}\,\delta\vec{\psi} + \mathbf{\Lambda^{-1}}\cdot\mathbf{L}^{-1}\,\vec{R}_A\,\delta A + \mathbf{\Lambda^{-1}}\cdot\mathbf{L}^{-1}\,\vec{R}_F\,\delta x \,, \tag{11}$$

where $\delta\vec{\xi}$ represents an arbitrary variation e.g. $\partial\vec{\xi}/\partial t$ or $\partial\vec{\xi}/\partial x$. Note that the variables *A* and *x* are not functions of time; cross-section variations due to the pipe elasticity are expressed with pressure variations. Introduction of modified characteristic variables (11) gives the characteristic-like form of Eq. (6):

$$\frac{\partial\vec{\xi}}{\partial t} + \mathbf{\Lambda}\frac{\partial\vec{\xi}}{\partial x} = 0 \,. \tag{12}$$

This equation represents the basis for the second-order accurate numerical scheme in the WAHA code. The discretisation of Eq. (12) was performed using the second-order accurate characteristic upwind discretisation (Hirsch, 1988):

$$\frac{\vec{\xi}_j^{\,n+1} - \vec{\xi}_j^{\,n}}{\Delta t} + (\mathbf{\Lambda}^{++})_{j-1/2}^{n} \frac{\vec{\xi}_j^{\,n} - \vec{\xi}_{j-1}^{\,n}}{\Delta x} + (\mathbf{\Lambda}^{--})_{j+1/2}^{n} \frac{\vec{\xi}_{j+1}^{\,n} - \vec{\xi}_j^{\,n}}{\Delta x} = 0 \ , \tag{13}$$

where subscripts $j,\ j \pm 1$ denote grid points of the spatial discretisation, subscripts $j \pm 1/2$ denote values between the grid points, Δx denotes distance between the two neighbouring grid points *j* and *j+1*, superscripts *n*, *n+1* denote time, and Δt time step i.e. an interval between time levels *n* and *n+1*. Elements of the diagonal matrices $\mathbf{\Lambda}^{++}$, $\mathbf{\Lambda}^{--}$ in Eq. (13) are calculated as:

$$\begin{aligned} \lambda_k^{++} &= |\lambda_k| \cdot f_k^{++} & f_k^{++} &= \max\left(0, \frac{\lambda_k}{|\lambda_k|}\right) + \frac{\phi_k}{2}\left(|\lambda_k|\frac{\Delta t}{\Delta x} - 1\right) \ , \quad k = 1,6 \\ \lambda_k^{--} &= |\lambda_k| \cdot f_k^{--} & f_k^{--} &= \min\left(0, \frac{\lambda_k}{|\lambda_k|}\right) - \frac{\phi_k}{2}\left(|\lambda_k|\frac{\Delta t}{\Delta x} - 1\right) \ , \quad k = 1,6 \end{aligned} \tag{14}$$

The first term of the factors f_k^{++} and f_k^{--} is the first-order upwind discretisation, and the second term with limiters ϕ_k is the second-order correction. The flux limiter ϕ_k can be chosen by the code user from the MINMOD, the Van Leer, or the Superbee limiter (LeVeque, 1992). The non-standard definition of the characteristic variables in Eq. (11) requires multiplication with the inverse matrix of the eigenvalues $\mathbf{\Lambda}^{-1}$. Computation of this matrix is not possible when any of the eigenvalues is equal to zero. To avoid this problem, the WAHA code calculates limiters ϕ_k from the following variables (see also Glaister, 1985):

$$\delta\vec{\zeta} = \mathbf{\Lambda} \cdot \delta\vec{\xi} = \mathbf{\Lambda} \cdot \mathbf{L}^{-1}\, \delta\vec{\psi} + \mathbf{L}^{-1}\vec{R}_A \delta A + \mathbf{L}^{-1}\vec{R}_F \delta x \ . \tag{15}$$

These new variables are then used to measure the ratio of the gradients in the flux limiters:

$$\theta_{k,j+1/2} = \frac{\zeta_{k,j+1-m} - \zeta_{k,j-m}}{\zeta_{k,j+1} - \zeta_{k,j}} = \frac{\Delta\zeta_{k,j+1/2-m}}{\Delta\zeta_{k,j+1/2}}, \qquad m = \frac{\lambda_{k,j+1/2}}{|\lambda_{k,j+1/2}|}, \ k = 1,6 \ . \tag{16}$$

The stability domain for the integration with the described scheme is limited by the Courant-Friedrichs-Levy (CFL) condition:

$$\Delta t \le \Delta x / \max(|\lambda_k|), \ k = 1,6 \, . \tag{17}$$

3.1 Evaluation of the Jacobian matrix

A simple average of the non-conservative variables is used for evaluation of the Jacobian matrix in Eq. (6) at the point $j+1/2$:

$$\mathbf{C}_{j+1/2} = \mathbf{C}[(\vec{\psi}_j + \vec{\psi}_{j+1})/2] \ . \tag{18}$$

A similar approach was taken by Gallouet and Masella (1996), who showed that this type of averaging gives very accurate results for Euler equations. They emphasized that the averaging (18) must be performed with primitive variables (pressures, velocities and densities). Another more complicated and possibly more accurate alternative was proposed by Toumi and Kumbaro (1996), which is not adopted in the present work. In attempt to evaluate the Roe's approximate

Riemann solver (Roe, 1981) for the six-equation Jacobian matrix $\mathbf{C}_{j+1/2}$, they proposed a rather complicated procedure for evaluation of the Jacobian matrix between the grid points j and $j+1$.

In the present numerical scheme, the same averaged variable

$$\vec{\psi}_{j+1/2} = (\vec{\psi}_j + \vec{\psi}_{j+1})/2, \tag{19}$$

is used to evaluate the non-relaxation source terms in the point $j+1/2$. Furthermore, the same type of averaging is used to evaluate the geometrical properties of the pipe (pipe cross-section and pipe inclination) at the point $j+1/2$.

3.2 Why non-conservative approach?

Numerous tests were performed with the six-equation model (described by Tiselj and Petelin, 1997) with different basic variables and the most successful set of variables turned out to be $\vec{\psi} = (p, \alpha, v_f, v_g, u_f, u_g)$. This set of variables is very close to the so-called primitive variables, where the phase internal energies u_f, u_g are replaced with the phase densities ρ_f, ρ_g. However, internal energies were retained due to the applied water property subroutines. The preferred set of variables would be a conservative form:

$$\vec{\varphi} = [(1-\alpha)\rho_f, \alpha\rho_g, (1-\alpha)\rho_f v_f, \alpha\rho_g v_g, (1-\alpha)\rho_f e_f, \alpha\rho_g e_g], \tag{20}$$

with specific total energy $e = u + v^2/2$. The conservative form of equations usually brings numerical conservation of mass, momentum and energy. However, there are some specific problems with the conservative formulation of multi-fluid two-phase flows:

1) The continuity and energy equations can be written in the conservative form, while the conservative fluxes for the momentum equations do not exist due to the pressure gradient terms, virtual mass terms, interfacial pressure terms, and possibly other correlations that contain derivatives. Thus, the momentum equations cannot be written in the conservative form.
2) If complex systems of equations are solved with the conservative variables (Tiselj and Petelin, 1997), oscillations appear in the vicinity of particular discontinuities. Abgrall (1996) explained such oscillations for the four-equation model (two continuity, one momentum and one energy equation). The oscillations do not depend on accuracy of the used numerical scheme and can be observed in the results of first- and the second-order schemes.
3) "Non-standard" water-vapour properties subroutines are required to calculate two-phase properties $(p, \alpha, \rho_f, \rho_g)$ from the conservative variables $((1-\alpha)\rho_f, \alpha\rho_g, (1-\alpha)\rho_f u_f, \alpha\rho_g u_g)$.

According to our experiences, the non-conservative variables present an acceptable approximation for fast transients. For long transients, where conservation of mass and energy is more important; this might be a serious drawback. In the test calculations presented by Tiselj and Petelin (1997, 1998) negligible fluctuations of the overall mass and energy (less than 2%) have been observed despite the non-conservative scheme. Some additional tests related to the behavior of the WAHA numerical scheme for the convective part of the equations with non-relaxation source terms are presented further in the text.

3.3 Test cases for the convective part of the equations

Ideal gas shock tube (Sod's problem) is the model of the Riemann problem model with pure single-phase gas. In order to estimate the errors due to the non-conservative numerical scheme, the calculations were performed with the WAHA code as well as with the conservative high-resolution shock-capturing scheme with the Roe's approximate Riemann solver. The modelled pipe has constant diameter and length of 10 meters. The wall friction, the inter-phase friction and the heat and mass transfer correlations are excluded from the calculation. The experiment starts at time $t = 0.0$ *s*, when the membrane that separates two different states in the pipe ruptures. The initial thermo-dynamical state is defined with three parameters: pressure, temperature and velocity. Left and right side initial conditions are taken from the Sod's work (1978): $p_L=10^5$ *Pa*, $\rho_L=1$ *kg/m*^{3}, $v_L=0$ *m/s*, $p_R=10^4$ *Pa*, $\rho_R=0.125$ *kg/m*^{3}, $v_R=0$ *m/s.*

Comparison with conservative scheme at time $t = 0.0061$ *s* is shown in Fig. 1. The solution obtained with conservative variables is practically equal to the analytical solutions, which are therefore not shown in Fig. 1. Non-conservative schemes are known to converge to a wrong solution when shocks are present in the flow field. However, in typical single-phase water hammer transients, the solution obtained with a non-conservative scheme is very close to the exact solution of the transport equations.. According to the results shown in Fig. 1, the non-conservative scheme does not seem to represent a big deficiency for most of the transients with shock waves in the gas phase, as long as the maximum to minimum pressure ratio is lower than approximately 10.

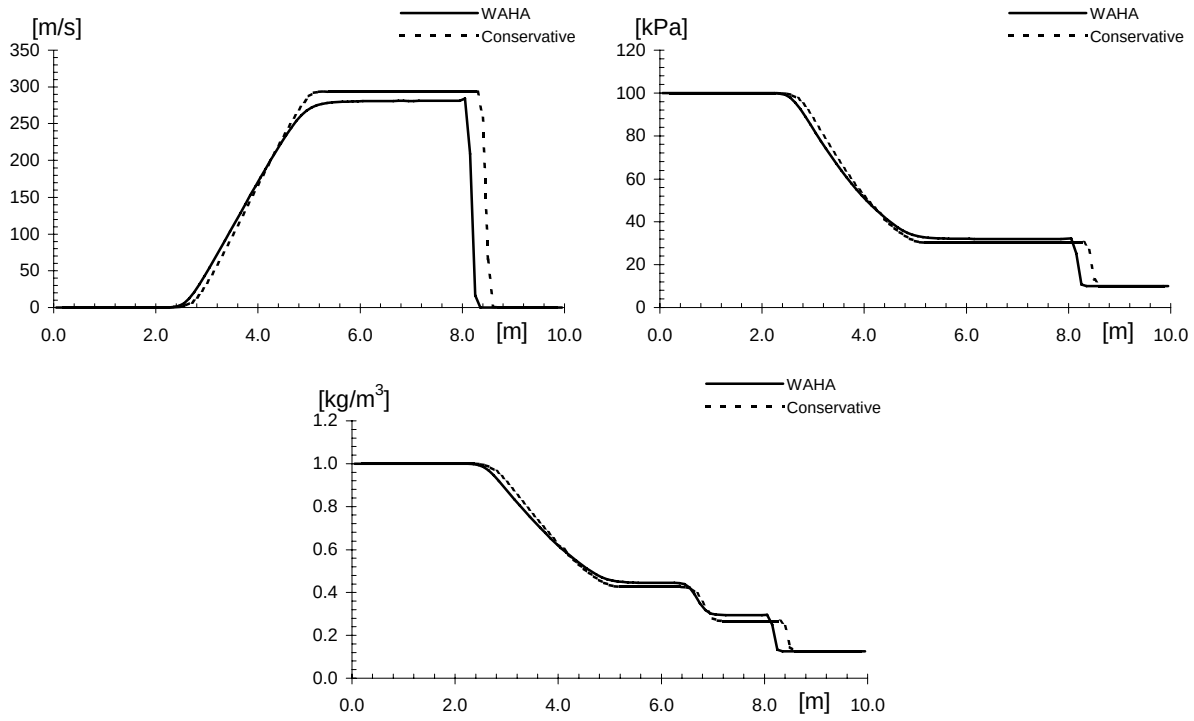

Figure 1: Pressure, velocity and density profiles, comparison of the WAHA code scheme and the conservative scheme results at time t = 0.0061 s.

Liquid shock tube is modelled in a pipe of constant diameter, length of 10 meters and closed ends on both sides. The wall friction, the inter-phase friction and the heat and mass transfer

correlations are excluded from the calculation. Beside calculations with the WAHA code, calculations with the conservative scheme were also performed. This comparison is an another test of (non)conservative properties of the WAHA code scheme.

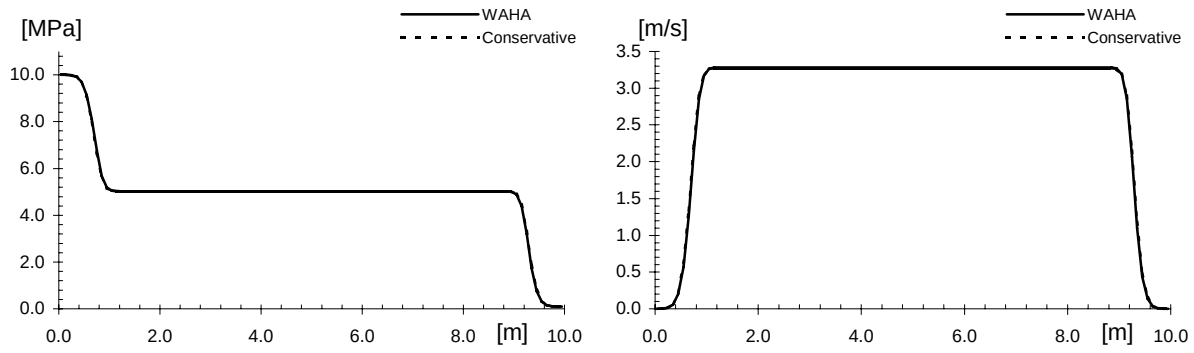

Figure 2: Pressure and velocity profiles calculated with the WAHA code scheme and the conservative scheme results at time t = 0.00285s.

The experiment starts at time t = 0.0 s when the membrane that separates two different states in the pipe ruptures. The initial thermo-dynamical state is defined with three parameters: pressure, temperature and velocity. At the beginning, a single discontinuity in form of a pressure drop from 100 to 1 bar is present in the pipe at 5 meters. The initial velocity is set to zero and the initial temperature is set to 300 K. Comparison with the conservative scheme at time t = 0.00285 s is shown in Fig. 2. There is practically no difference between the non-conservative WAHA code scheme and the results of the test code with the conservative variables, despite the very strong initial pressure discontinuity. Relative mass and internal energy non-conservation is less than 10^{-7}. Thus, the influence of the non-conservation approach is negligible in the case of single-phase liquid shock waves for all practical pressure drops.

Critical flow of ideal gas in convergent-divergent nozzle is modelled in a pipe of variable cross-section with length of 3.226 meters (convergent-divergent part is 3 m long) and constant pressure on both sides. The case is used to test the performance of the WAHA code numerical scheme in the variable cross-section geometry, i.e. to test of the non-relaxation source terms responsible for the cross-section variations. Geometry and boundary conditions are taken from the book of Anderson (1995). The nozzle has equal inlet and outlet cross-sections with the minimum cross-section 6 times smaller than the inlet cross-section. Boundary conditions are defined with constant pressure. Pressure on the left side is $p_L = 1\ bar$ and on the right side is $p_R = 0.6784\ bar$. The initial velocity is set to zero, initial temperature is set to $T = 300\ K$ and initial pressure in the nozzle is $p = 1\ bar$.

Beside the calculations with the WAHA code, the calculations with the test code using the conservative variables were also performed. The transient calculations were stopped when the steady state was achieved.

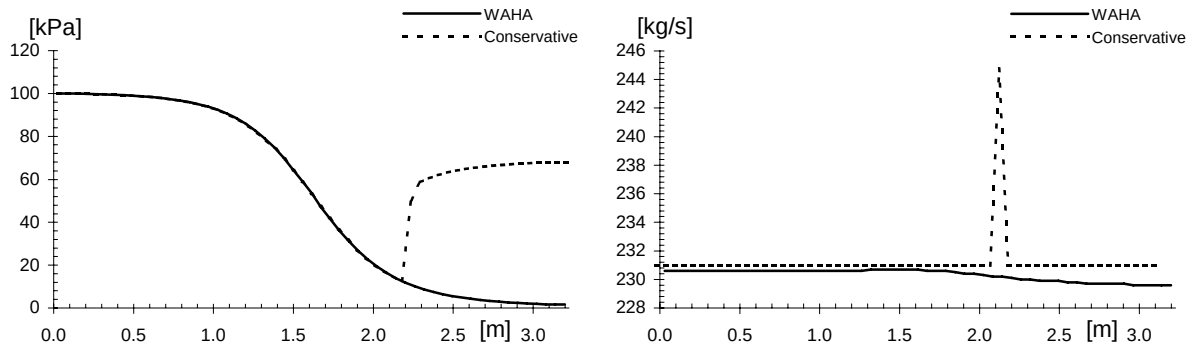

Figure 3: Steady-state flow in convergent-divergent nozzle, comparison of the WAHA code scheme and the conservative scheme results.

Steady-state conditions are established after approximately 0.1 s. Figure 3 shows steady-state pressure, velocity, and mass flow rate profiles . The results of the conservative scheme are practically the same as the analytical solutions of the steady-state problem (0.1% difference in the mass flow rates). The conservative profile of the mass flow rate shows a spike in a single volume, which lies within the shock wave in the divergent part of the nozzle. This spike is due inability of the conservative scheme to predict the position of the shock with accuracy greater than the length of a single control volume. This discrepancy becomes zero only when the shock position is exactly between two discrete points.

As seen in Fig. 3, the WAHA code predicts the correct critical mass flow rate, however, it fails to predict the stationary shock where supersonic to subsonic transition takes place in the divergent section of the nozzle. The conservation of mass (energy, momentum) is accurate to 0.5% as long as there are no stationary shocks in the solutions. As such shocks do not appear in two-phase critical flows (see critical flow cases in the paper by Gale et. al., 2006) and in critical flows of pure liquids, this deficiency does not seem to present a large limitation for the WAHA code.

Oscillations of the liquid column in the U-shaped pipe. The U-shaped pipe is partially filled with water and ideal gas (case 1) or vapor (case 2) with its boundaries sealed. The modelled pipe has constant cross-section and length of 20 meters. The wall friction is excluded from the calculation, while the basic WAHA inter-phase friction correlation for thermal equilibrium flow are applied in the first case and basic WAHA correlation for gas-liquid flow in the second case. The initial conditions are set for pressure to $p = 1.0$ *bar*, for liquid velocity to $v_l = 2.1$ *m/s*, and for temperature to $T = 373.1$ K. Figure 4 shows the initial position of the slug at time $t = 0.0$ *s*. The pipe is initially half filled with water and initial velocity gives disturbance into the system. The first graph in Fig. 4 shows deformation of the slug due to the initial thermal instability and due to the transport. It also shows comparison of results from two different models, the gas-liquid model and the vapor-liquid model, after 30 s of real time. Graphs in Fig. 5 show velocity history at the middle of the pipe (bottom). After 30 seconds of the transient, mass and total energy non-conservation for the vapor-liquid case is 0.03% and 0.4%, respectively, and 0.1% and 1.2% for the gas-liquid case.

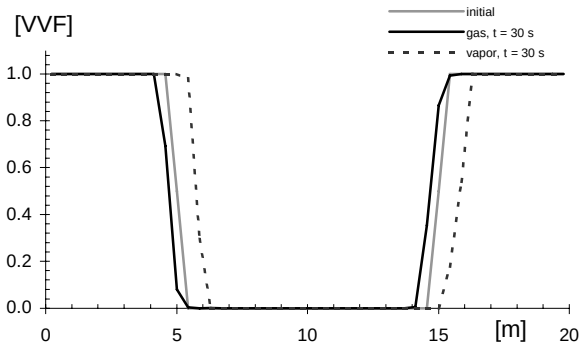

Figure 4: Vapor and gas volume fractions at t = 30 s

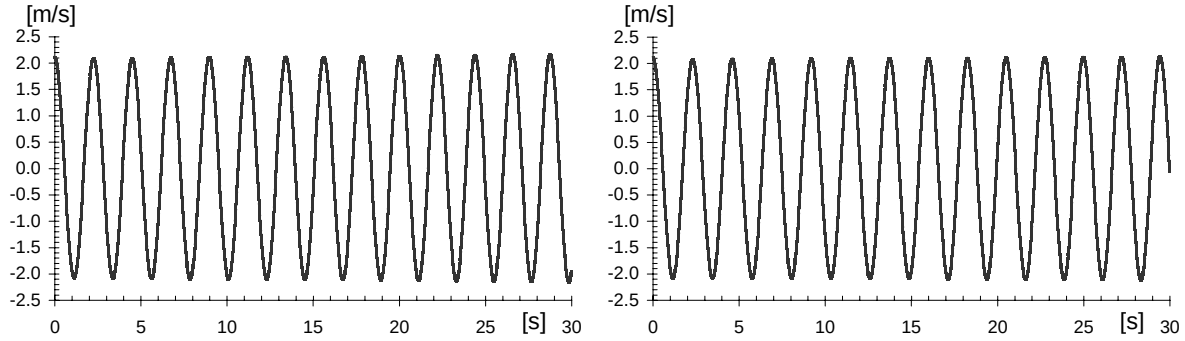

Figure 5: Vapor (left) and gas (right) velocity history at the bottom of the U-tube.

"Dam-break" problem in the horizontal pipe has been modelled in a pipe with constant cross-section and length of 2.0 meters. The pipe is closed on both ends. Liquid and gas phase are initially separated with a dam (membrane) in the middle of the pipe, which breaks at time *t = 0.0 s*. The inter-phase heat and mass transfer are excluded from the calculation (i.e. ideal gas option is applied). The initial conditions along the pipe are constant with pressure *p = 1.0 bar*, velocity *v = 0.0 m/s* and temperature *T = 300 K*.

In the first dam-break problem, the vapor volume fraction on the left side of the dam is $\alpha_L=0.501$ and slightly lower on the right side $\alpha_R=0.5$. This case was used to compare the calculated speed of the small surface waves in shallow water with the theoretical value, which is $v_t = \sqrt{h\,g} = 0.74 m/s$ (where *h* presents the liquid depth and *g* gravitational acceleration). For vapor volume fraction $\alpha=0.5$, the liquid depth is equal to the pipe radius, which is obtained from the pipe cross-section $A = 0.01\ m^2$. Rough estimation of the wave speed from WAHA results, where the left and the right waves passed a distance of 0.37 (±0.01) m in 0.5 s, is 0.74 m/s, which is equal to the theoretical prediction.

In the second dam-break problem, the left and right vapor volume fractions are $\alpha_L = 1.0$ and $\alpha_R = 0.0$. Figure 6 below shows the results of the second dam-brak problem. After the dam breaks, water in the pipe starts to oscillate i.e. waves are being reflected from the closed ends. The horizontally stratified stagnant state is achieved after sufficiently long time, due to the dissipation of the momentum through the wall friction. Mass and total energy non-conservation during the first 5 seconds of the transient is 0.01% and 0.4%, respectively.

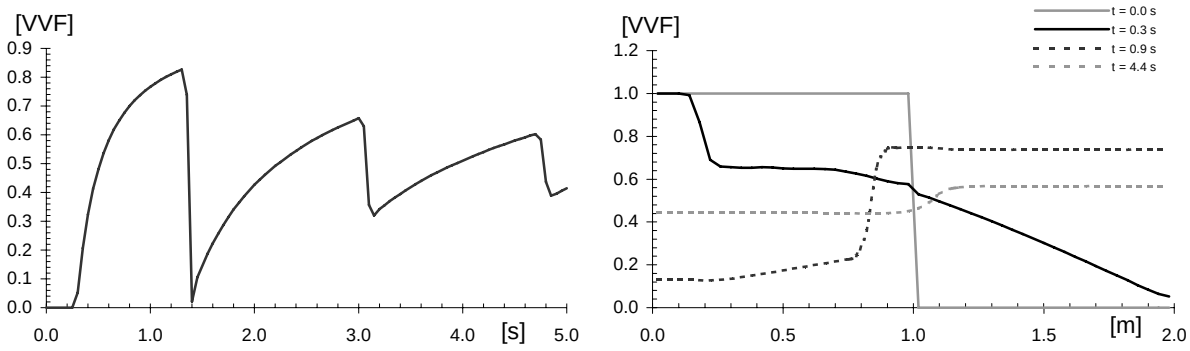

Figure 6: Vapor volume fraction history in the middle of the pipe and vapor volume fraction profiles at different times.

4. Integration of the relaxation source terms

In the second sub-step of the operator splitting scheme, Eq. (4), is integrated over the convective time step Δt with the first-order explicit method at each grid point. Time steps of the integration depend on the stiffness of the relaxations and can be much shorter that the main time step Δt. First-order accuracy of this sub-step is compensated by the shorter time steps in integration of Eq. (4).

Another option, which is available in the WAHA code, is instantaneous relaxation of the source terms in Eq. (4). In this case, it is assumed that the inter-phase exchange processes are infinitely fast. Integration of Eq. (4) with infinite values of inter-phase friction *(C_i)*, and liquid-interface and gas-interface volumetric heat transfer coefficients (H_{if}, H_{ig}) is not possible. However, the relaxed state can be found directly as the both phase velocities become equal to the mixture velocity and the phase properties (densities, internal energies) become equal to the equilibrium properties. The properties of the thermal equilibrium are calculated from the given mixture density and the mixture internal energy.

The relaxation source terms of the two-fluid model do not affect the properties of the mixture at a given point; mixture density ρ_m, mixture momentum $v_m \rho_m$, and mixture total energy $e_m \rho_m$ should remain unchanged after the integration of the relaxation source terms. In principle it is possible to choose a set of basic variables $\vec{\psi}_M = (\rho_m, v_m \rho_m, e_m \rho_m, v_g - v_f, T_f, T_g)$, that enables simplified integration of the relaxation source terms. If $\vec{\psi}_M$ is chosen as a vector of basic variables, only a system of three differential equations is solved instead of the system of six differential equations, because there are no relaxation source terms for the first three components of the vector $\vec{\psi}_M$. This reduction of the system is only partially taken into account in the WAHA numerical scheme. Only one relaxation equation for the inter-phase friction is solved for the relative velocity $v_r = v_g - v_f$. Subsequently, the phase velocities are calculated from the relaxed relative velocity v_r and the known mixture velocity v_m , which remains unchanged. Similar reduction of the thermal relaxation source terms is not used, because it is difficult to calculate the fluid state (pressure p and vapor volume fraction α) from the variables $(\rho_m, e_m \rho_m, T_f, T_g)$ that are result of such relaxation. The problem is similar as in the case of the conservative variables, which are also not very convenient input for the water

properties. Thus, thermal relaxation in the current version of the WAHA code is calculated with variables (p, α, T_f, T_g).

The time step for the integration of the source terms Δt_S is not constant and is controlled by the relative change of the basic variables. Currently, the maximal relative change of the basic variables in a single step of the relaxation source term integration is limited to 0.01 in order to obtain results that do not depend on the numerics. When it is necessary, the time step Δt_S is further reduced to prevent the sign change of temperature differences $T_f - T_s$ and $T_g - T_s$, where T_s is the saturation temperature at given pressure. If sign change is encountered, the new values are discarded, the time step is halved and new values are calculated again with the halved time step. If the time step Δt_S drops below 10^{-19} s, the integration is interrupted and the code stops issuing a failure message. If the steam or liquid volume fractions drop below $\varepsilon = 10^{-12}$, the relaxation is also stopped as one of both phases disappeared.

Source terms describing inter-phase exchange are weak when the two-phase mixture is close to thermal and mechanical equilibrium. In that case the time step for their integration Δt_S is equal to the convection time step Δt. When the mixture is far from equilibrium, the source term integration time step Δt_S can be a few orders of magnitude shorter that Δt. As a consequence a few hundred or thousand sub-steps can be required to integrate the relaxation sources over a single convection time step Δt.

As long as either vapor or liquid volume fraction is smaller than 10^{-6}, the WAHA code uses instantaneous thermal and mechanical relaxation. In other words, homogeneous-equilibrium mixture is assumed in such conditions. As the vapor or the liquid volume fraction grows over that limit, the WAHA code starts with application of the relaxation process described above

Possible further work in the field of the relaxation source terms integration is the implementation of the implicit time advancement, which would be faster than the current explicit procedure.

Two-phase shock tube test case. Part of the results in this section can be reproduced only with modification of the WAHA source code, where the fixed values are chosen for the coefficients C_i, H_{if} and H_{ig} of the inter-phase heat, mass, and momentum exchange source terms. Results without relaxation source terms and with infinitely fast relaxation can be obtained without modification of the WAHA source. The case was developed to test the procedure for the integration of the relaxation source terms. Detailed discussion and more results can be found in Tiselj et. al. (2003). Two-phase shock-tube is the Riemann problem for the two-fluid model, i.e. a single discontinuity in 1D. Results in Fig. 8 and Fig. 9 are for the following initial conditions:

$x < 50$ m: $p = 15$ MPa, $\alpha = 0.1$, $v_f = v_g = 0.0$, $T_f = T_g = 615.3$ K
$x > 50$ m: $p = 10$ MPa, $\alpha = 0.5$, $v_f = v_g = 0.0$, $T_f = T_g = 584.2$ K

As can be noticed, the phasic temperatures and phasic velocities on both sides are equal, thus the initial state can be used as an input for the six-equation WAHA model and also for the three-equation Homogeneous Equilibrium Model (HEM). The HEM results in this section are obtained with similar numerical scheme as the WAHA code results, but with the conservative variables.

Figure 7 presents a series of five simulations with the two-fluid model (WAHA code) and one simulation with the HEM model, on a grid with 100 nodes. The results are presented at time $t=0.081\ s$. Calculations with the two-fluid model were performed using various constant values of the coefficients C_i, H_{if} and H_{ig}. Values of the coefficients are written in each graph of the Fig. 7. The stratification factor was set to $S = 0$, i.e., the virtual mass term was used in equations, while the interfacial pressure was zero. It is important to stress that virtual mass presents significant inter-phase friction, which is present in all simulations. The phasic velocities are shown in the left and the phasic temperatures in the right column of the Fig. 7. No inter-phase exchange was allowed in the first simulation (first row in Fig. 7). One can see a significant difference between the solutions of the two-fluid model and the solutions of the HEM model. Shocks traveling right and rarefaction waves traveling left are much faster in two-fluid model than in the HEM model. Discontinuity in the middle of the tube, which exists in the two-fluid model solutions, does not exist in the HEM solutions. Larger coefficients are used in the next simulation (second row in Fig. 7). One can see that the phasic velocities are closer, while the phasic temperatures are still far away. In the third simulation (third row in Fig. 7), the phasic velocities are quite close, while differences in the temperatures are still significant. Here it can be seen that discontinuities of the two-fluid model become smeared; instead of the sharp shocks, rarefaction waves and contact discontinuities, the waves are interlaced. The phasic velocities and temperatures are very close together in the fourth simulation (fourth rows in Fig. 7) and also close to the solutions of the HEM model. When the coefficients are increased further (bottom row in Fig. 7), a two-fluid model with extremely high inter-phase mass, momentum and energy transfer is obtained. Such two-fluid model is practically equal to the three-equation HEM model. Results obtained with $C_i = 10^6$ and $H_{if} = H_{ig} = 10^9$ are practically the same as results obtained with infinite values of the coefficients.

Pressure and vapor volume fractions are presented in Fig. 8 only for the two limiting cases:

- infinitely fast relaxation (WAHA – HEM),
- no relaxation.

It can be noticed in the bottom row of Fig. 7 that solution of the WAHA code with very large values of coefficients is more "diffusive" than the HEM solution. This is due to the non-accuracy of the operator splitting technique (see Section 2 and Tiselj et. al. 2003).

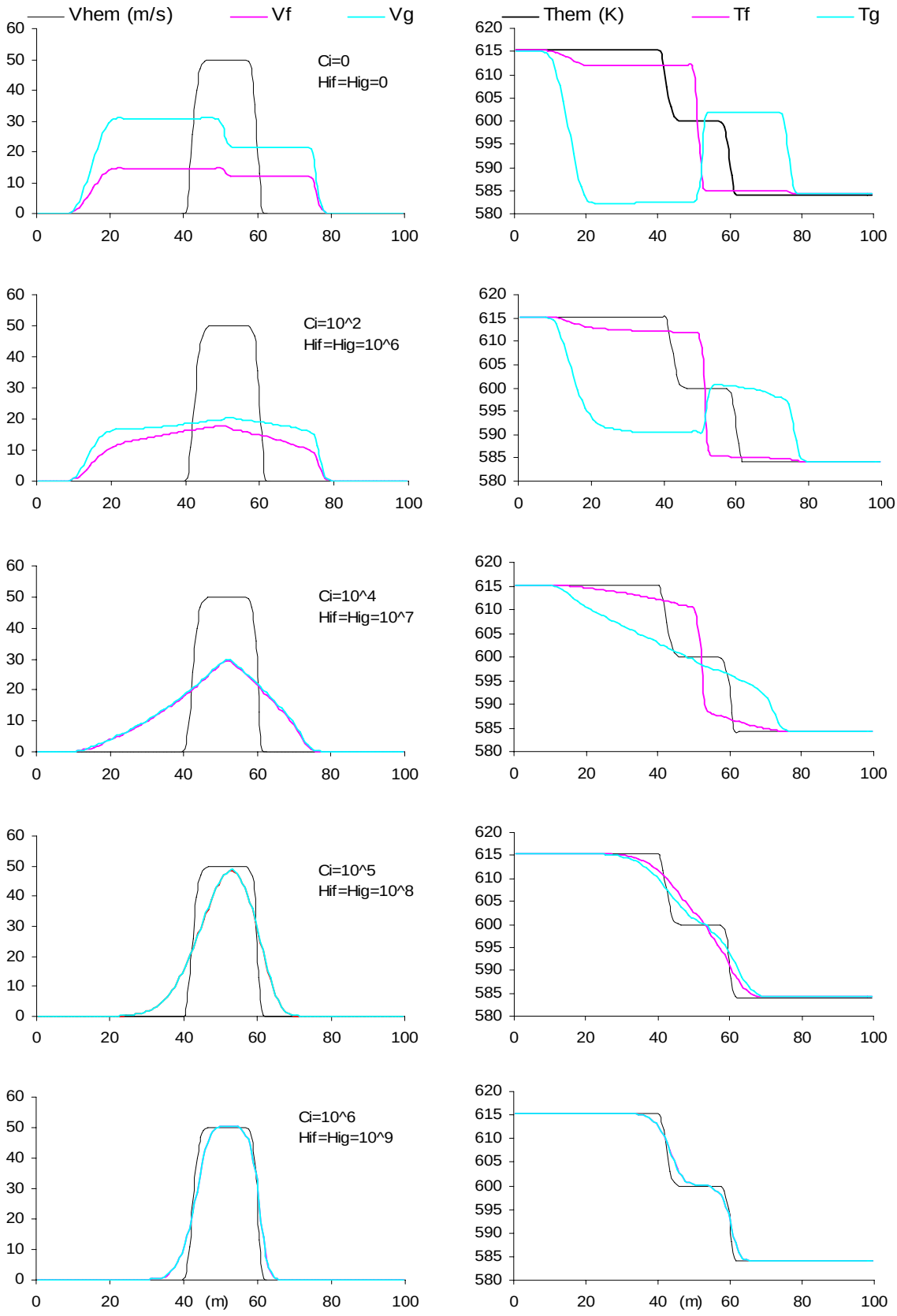

Figure 7: Shock-tube velocities v_f, v_g and temperatures T_f, T_g of the HEM model and two-fluid model with various inter-phase drag (C_i) and heat transfer coefficients (H_{if} , H_{ig}).

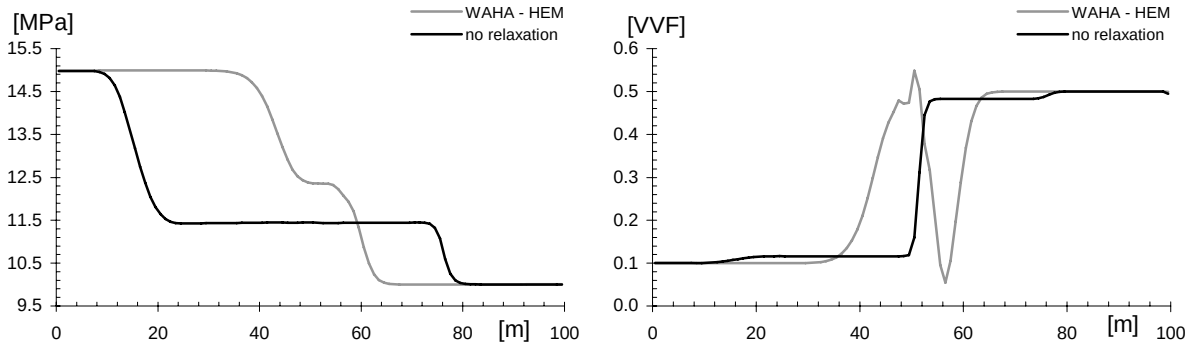

Figure 8: Pressure and vapor volume fraction profiles at t = 0.081 s predicted by WAHA with instantaneous relaxation (HEM - grey) and without any relaxation (no relaxation - black).

5. Single-phase to two-phase and two-phase to single-phase transition

Single-phase flow in the WAHA code is modelled as two-phase flow with volume fraction of the non-existing phase set to $\alpha_{RESIDUAL} = \varepsilon = 10^{-12}$. As six eigenvalues and eigenvectors are also defined in single-phase flow volumes, this approach automatically saves the problem with convection of two-phase flow into the volume previously filled with single-phase flow.

The problem of transition from single to two-phase flow (or reverse) during the convective sub-step of the operator-splitting scheme is the negative vapor volume fraction or the vapor volume fraction larger than 1.0 that can appear within the applied numerical scheme. The problem of $\alpha < 0$ or $\alpha > 1$ is solved with a patch that modifies flux of α when it falls out of its bounds. Treatment of the negative vapor or liquid volume fractions in the WAHA code decreases accuracy of the numerical scheme, as it is a source of certain mass and energy non-conservation (see details in Tiselj et. al. 2004). Single to two-phase flow transition often occurs in the U-tube simulations described in Section 3. In this case, it is responsible for the major part of the mass and total energy non-conservation.

Separation of liquid and vapor in a vertical pipe is a hypothetical test case where the two-phase to single-phase transition plays an important role. The pipe has length of one meter and has two closed ends The initial conditions represent homogeneously mixed liquid and vapor. The pipe has constant initial vapor volume fraction $\alpha = 0.52$, pressure $p = 0.9$ *bar*, velocity $v = 0.0$ *m/s*, and temperature $T = 370$ *K*, along the pipe. Separation proceeds due to gravity. The WAHA correlations are applied for inter-phase heat, mass and momentum transfer. Liquid and vapor are separated in a few seconds. Graphs in Fig. 9 show the final steady-state distribution of the pressure and of the vapor volume fraction. Non-conservation of mass in the WAHA calculation is approx. 2%, which is more than in the other transients described before. Another weakness is exhibited in the code when the Van-Leer or the Superbee limiters are chosen; the separation test does not reach the expected steady-state. Thus, it is recommended to use the MINMOD slope limiter in all the WAHA code calculations.

Steam appearance due to flashing. Flashing starts when pressure of a single-phase liquid drops below the saturation pressure. The subroutine *flash* is called just before the relaxation source term sub-step if the flow in the cell is a single-phase liquid and the pressure is lower than the saturation pressure at current liquid temperature. The process starts as a homogeneous-equilibrium process. A possible improvement of the flashing model is the use of flashing delay models.

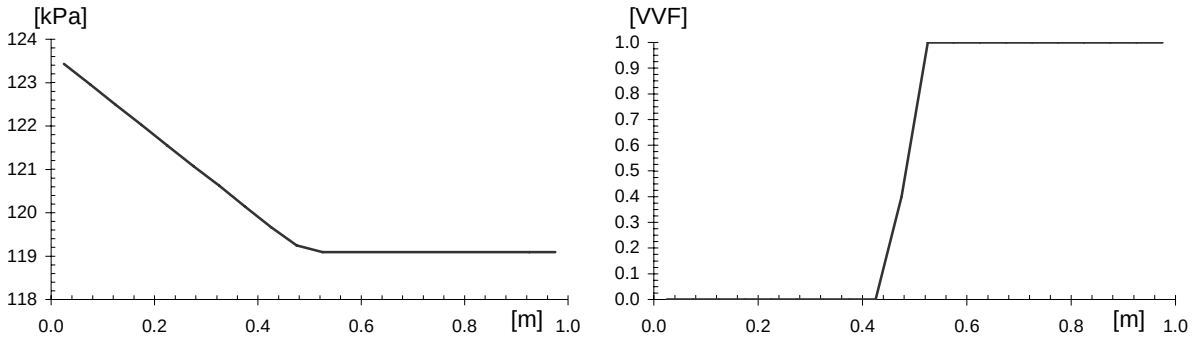

Figure 9: Steady-state pressure and vapor volume fraction distribution after the separation of liquid and vapor mixture.

Liquid appearance due to the onset of the condensation. Condensation starts in pure vapor when pressure increases above the saturation pressure at current vapor temperature. The process starts as a homogeneous-equilibrium process.

Disappearance of the liquid/steam due to the vaporization/condensation. Disappearance of a particular phase is similar to its generation. When vapor or liquid volume fraction drops below the value 10^{-6}, the homogeneous-equilibrium assumption is used instead of the relaxation correlations. Instantaneous equilibrium can automatically change the flow from two-phase to single-phase.

6. Water properties of the WAHA code

WAHA water properties are tabulated with a separate program and stored in a table. The WAHA subroutines determine the properties with interpolation from that table. Dynamic viscosities, thermal conductivities and surface tension are obtained directly with interpolating functions from separate subroutines. The table with water properties was created with software from UCL (Seynhaeve et al. 1992) and it also contains description of the metastable states (superheated liquid and subcooled vapor).

Vapour and/or liquid densities, and specific internal energies are tabulated for each chosen temperature and pressure:

Temperatures:
- $T_1 = 273.15\ K$,....., $T_{NTP} = 647.15\ K$, increment $1.0K$, i.e. $NTP=375$ - **two-phase area**
- $T_{NTP+1} = 648.15\ K$,....., $T_{NT} = 1638.15\ K$, increment $10.0\ K$, i.e., $NT = 475$

Pressures:
- $p_0=-95.0\ bar$,
- $p_1 = 0.00611\ bar$,..., $p_{NTP} = 220.55\ bar$, two-phase area: each pressure is evaluated as a saturation pressure at the corresponding temperature: $p_j = p_{sat}(T_j)$,
- $p_{NTP+1}=221.0bar$, ..., $p_{NTP+8}=291.0bar$, increment $10.0\ bar$, $p_{NTP+9}=350.0\ bar$, $p_{NTP+10}=400.0\ bar$, ... $p_{NTP+16}=1000.0\ bar$, increment $100.0\ bar$.

The number of pressures p_j in the two-phase area is exactly the same as the number of temperatures *NTP*. Each pressure p_j is evaluated as a saturation pressure p_{sat} at the corresponding temperature T_j, with $p_1 = 0.00611$ *bar* and $p_{NTP} = 220.55$ *bar*. Practical side of this choice is calculation of the saturation properties with exactly the same subroutines as the single-phase properties. Namely, arbitrary property can be calculated for a point (T_i,p_j) and the saturation conditions are stored at $i = j$.

There is one negative pressure value at which the metastable liquid properties are defined at temperatures from *273.15* to *647.15 K*. As negative pressures occur very rarely, but might be still reached for a very short time during some water hammer transients, this simple extension of the water property tables prevents the calculation to crash if negative pressure is encountered in single phase liquid.

For the input (*p,u*) or (*p,T*), the WAHA code water property subroutines find the three tabulated neighbours (p_1,T_1), (p_2,T_2), (p_3,T_3), which define a triangle that surrounds the point (p,u) or (p,T). Equation of a plane is found for the given three points as a function of pressure and temperature, e.g. for internal energy: $u = k\,p + m\,T + n$, where the values of derivatives $k = (\partial u/\partial p)_T$, and $m = (\partial u/\partial T)_p$ have to be found. Similar linear equation is determined for density ρ. When internal energy is given as an input instead of temperature, the equation of plane is still formed as $u = k\,p + m\,T + n$ and temperature T calculated from it. This approach ensures that results of the two consecutive calls $u_0 = u(p_0, T_0)$ and $T_1 = T(p_0, u_0)$ are identical.

The values of derivatives could also be tabulated and later calculated with interpolation, however such water property subroutines are not consistent and were found to cause larger non-conservation of mass and energy. Thus, this approach is not recommended.

The implemented of water property interpolation means that the main variables ρ, u are continuous, piecewise linear functions of T and p and vice versa, with discontinuous first derivatives at the boundaries of the triangles specified by the points (p_i, T_j). The derivatives of the main parameters T, p, ρ, u, are piecewise constant inside each triangle and discontinuous at the triangle boundaries. Sonic velocity, which is calculated from the derivatives, is also discontinuous at the boundaries of the triangles. However, as the tabulated densities for (p_i, T_j) points is rather fine, this does not present a problem for the WAHA code.

Verification of the WAHA steam tables was performed with one of the earliest versions of WAHA code (version WAHA0 from 2002) with the WAHA steam tables, and the same WAHA code, but with the steam tables of RELAP5/MOD3.2.2 Gamma. Results of the comparison for the liquid and the vapour shock tube and for the Edwards pipe experiment (Edwards, O'Brien, 1970) can be found in the WAHA manual (Tiselj. et. al., 2004).The differences are practically invisible in the graphs, while the code is running roughly two times faster with the WAHA water property subroutines.

7. Models of two-phase flow through sudden expansion, contraction, or branch

This chapter gives a description of special models implemented in the WAHA code to simulate single and two-phase flow through an abrupt area change in a pipe. The second part of the chapter describes model of the branch, which is built on the abrupt area change model.

The models were tested for the flow through a pipe expansion and a contraction. The results of single phase flow simulations were compared with analytical solutions and results obtained by the RELAP5 code.

7.1 Abrupt area change model

The abrupt area change model is needed, when flow passes through a sudden expansion or a contraction area in a channel. In that case, the transport equations cannot correctly model the physical situation, despite the variable pipe cross-section model used in the WAHA equations (see Section 2). The variable pipe cross-section model of the WAHA code is suitable if the contraction or expansion over the pair of neighbouring grid points of the pipe represents a small fraction (~10%) of the pipe cross-section. When the cross-section of the pipe is suddenly increased or decreased for a factor larger than approximately 2, it is more reliable to use an abrupt area change model.

The implemented abrupt area change model is built on 3 basic assumptions:

- steady-state balance conditions for conservative variables φ across the area change (marked with $k \rightarrow n$),
- no generation (or loss) of mass, momentum and energy at the surface,

$$\left.\frac{\partial \vec{\varphi}}{\partial x}\right|_{k\rightarrow n} = 0 \ . \tag{21}$$

- preservation of characteristics ξ in each pipe,

$$\left.\frac{d\vec{\xi}}{dt}\right|_{k} = 0 \quad \text{and} \quad \left.\frac{d\vec{\xi}}{dt}\right|_{n} = 0 \ . \tag{22}$$

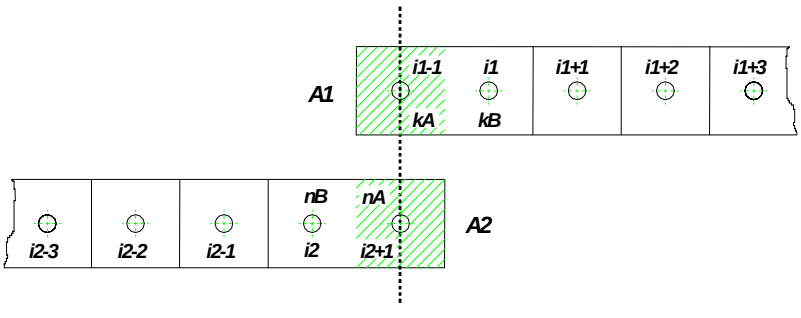

Figure 10: Grid point arrangement for the conservative-characteristic abrupt area change model with the ghost nodes *kA* and *nA*.

Figure 10 shows the numerical grid used for the calculations. A ghost cell is attached to each end of the pipe and is used to prescribe the appropriate boundary condition. The numerical

algorithm checks all pipes and calculates the junction relations between the pipe *k* and the neighbouring pipe *n*. The conservative-characteristic model implements the conservation relations (21) between the ghost grid point *kA* and the ghost grid point *nA*. It also uses the relations (22), which extrapolate characteristic ξ from the regular grid point *kB* or *nB* in the flow direction, if ξ is positive, and in the opposite direction, if ξ is negative. Using extrapolation of the positive characteristics ξ from the grid point *nB* to *nA* and of the negative characteristics ξ from the grid point *kB* to *kA*, the discrepancy vector *F* is defined as:

$$\begin{aligned} &\text{if } \lambda_j \geq 0 \quad F_j = \tilde{L}_{ji}^{-1} \left({}^{it}(\psi_i)_{kA} - (\psi_i)_{kB} \right) \qquad j = 1,...,6 \\ &\text{else} \qquad\quad F_j = \tilde{L}_{ji}^{-1} \left({}^{it}(\psi_i)_{nA} - (\psi_i)_{nB} \right) \end{aligned} \tag{23}$$

The steady-state balance conditions for the conservative variables φ are then written between the grid points *kA* and *nA* as:

$${}^{it}(\varphi)_{kA} - {}^{it}(\varphi)_{nA} = F_j \ , \qquad j = 7,...,12 \tag{24}$$

with arithmetic averaging of the non-conservative pressure gradients. By expressing the conservative variables with non-conservative $\varphi = \varphi(\psi)$, the discrepancy vector was minimized using the Newton-Raphson method:

$$\begin{aligned} {}^{it}(\psi_j)_{kA} &= {}^{it-1}(\psi_j)_{kA} - {}^{it-1}\left[\frac{F_j}{(\partial F_j / \psi_i)_{kA,nA}} \right] , \qquad j = 1,...,12 \quad \text{and} \quad i = 1,...,6 \\ {}^{it}(\psi_j)_{nA} &= {}^{it-1}(\psi_j)_{nA} - {}^{it-1}\left[\frac{F_j}{(\partial F_j / \psi_i)_{kA,nA}} \right]. \end{aligned} \tag{25}$$

The iteration procedure is stopped when

$$err = \sum_{j=1}^{6} \left({}^{it}(\psi_j)_{kA} - {}^{it-1}(\psi_j)_{kA} \right) + \left({}^{it}(\psi_j)_{nA} - {}^{it-1}(\psi_j)_{nA} \right) < 10^{-7} \ . \tag{26}$$

It is important to note that the momentum balance in the point of the area change applied in the conservative-characteristic abrupt area change model is not the same as the momentum balance of the basic two-fluid model of the WAHA code. Namely, special terms like virtual mass term and interfacial pressure term are not taken into account in the momentum balance used in an abrupt area change model. On the other side, the characteristic variables are obtained from the basic two-fluid model of the WAHA code. Detailed description of the procedure is given in the manual of the WAHA code (Tiselj et. al. 2004).

At the end of each time step, the junction models are introduced to calculate values of the primitive variables p, α, v_l, v_g, u_l, u_g in the ghost grid points *kA* and *nA*.

Single-phase shock tube with an abrupt area change - contraction - liquid. The case represents liquid flow through a contraction modeled with an abrupt area change model. The modelled pipe has length of 5 meters, closed end on both sides (boundary conditions are irrelevant as the results are being taken before the waves reach the pipe ends) and an area change with a contraction factor $A_1/A_2 = 20$, at distance 3 meters from the beginning. The wall friction and momentum losses at the contraction are excluded. Although, the case is not very realistic, such results can be compared with analytical results derived for the low velocities. The numerical experiment starts at time t = 0.0 s when the membrane, which separates two different

states in the pipe, is ruptured. The initial thermo-dynamical state is defined with pressure, temperature and velocity:

A_L=0.4 m^2, p_L=1.0 10^7 Pa, v_{fL}=v_{gL}=0, T_{fL} =584.2 K
A_R=0.02 m^2, p_R=0.5 10^7 Pa, v_{fR}=v_{gR}=0, T_{fR}=584.2 K

Initial discontinuity is present at a position of 2 meters.

Three different curves are shown in each graph of Fig. 11. The first line shows initial conditions, the second curve at *t = 0.0004 s* shows the shock wave travelling toward the contraction, and the third curve shows the behaviour of the transmitted and reflected waves. Our concern is behaviour of the waves after the rupture of the membrane and after the entrance into the contraction. The reflected and transmitted waves are clearly seen in Fig. 11. Their magnitude is in agreement with equations derived from the Joukovsky theory (Martin, Wiggert, 1996), which predicts the "transmittance" factor:

$$s = \frac{p'' - p_0}{p' - p_0} = \frac{2A_1 / c_1}{A_1 / c_1 + A_2 / c_2}\,, \tag{27}$$

where p_0 presents the initial pressure at the contraction, p' is the pressure of the incident wave, p'' the pressure of the transmitted wave, and c_1, c_2 are sonic velocities, which are equal in this case. The theoretical pressure p'' after the contraction obtained from the equation (27) is:

$$\left.\begin{aligned} p' &= 74.9\ bar \\ p_0 &= 50.0\ bar \end{aligned}\right\} \quad \Rightarrow \quad p'' = 97.4\ bar\,. \tag{28}$$

The WAHA code calculates p''_{WAHA} = 97.6 *bar*.

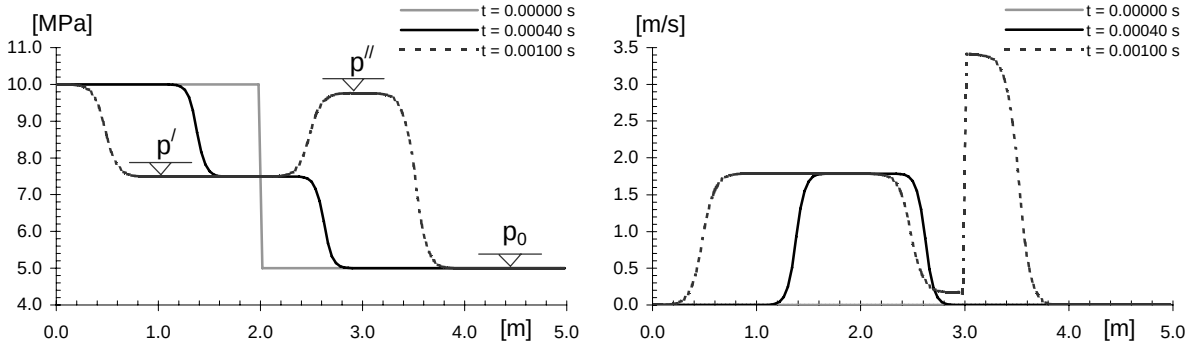

Figure 11: Pressure and velocity profiles at different time.

Single-phase shock tube with an abrupt area change - expansion - vapor. The modelled pipe has length of 5 meters, closed ends and an area change with the expansion factor A_2/A_1 = *20*, at distance 3 meters from the beginning. The wall friction is excluded in order to allow comparison with analytical results. The numerical experiment starts at time *t = 0.0 s* when the membrane at position 2 meters from the beginning, which separates two different states in the pipe, is ruptured. The initial thermo-dynamical state is defined with pressure, temperature and velocity:

A_L=0.02 m^2, p_L=1.5 10^7 Pa, v_{fL}=v_{gL}=0, T_{fL} =644.17 K
A_R=0.4 m^2, p_R=1.0 10^7 Pa, v_{fR}=v_{gR}=0, T_{fR}=607.96 K

There are three different curves shown in each graph of Fig. 12. The first line shows initial conditions, the second curve at $t = 0.0008\ s$ shows the shock wave travelling toward the expansion, and the third curve shows the behaviour of the transmitted and reflected waves. Our concern is behaviour of the waves after the rupture of the membrane and after the entrance into the expansion. The reflected and transmitted waves are clearly seen in Fig. 12. The results obtained with the Joukovsky equation (27) (Martin and Wiggert, 1996) give pressure p'' :

$$\left.\begin{aligned} p' &= 122.1\ bar \\ p_0 &= 100.0\ bar \end{aligned}\right\} \quad \Rightarrow \quad p'' = 102.1\ bar\ . \tag{29}$$

The WAHA code calculates $p''_{WAHA} = 102.0\ bar$. In derivation of the Joukovsky equation, it is assumed that fluid velocity is much smaller than the local speed of sound, and the density is constant. The assumptions are responsible for a small pressure jump that exists at the discontinuity after the reflection of the wave.

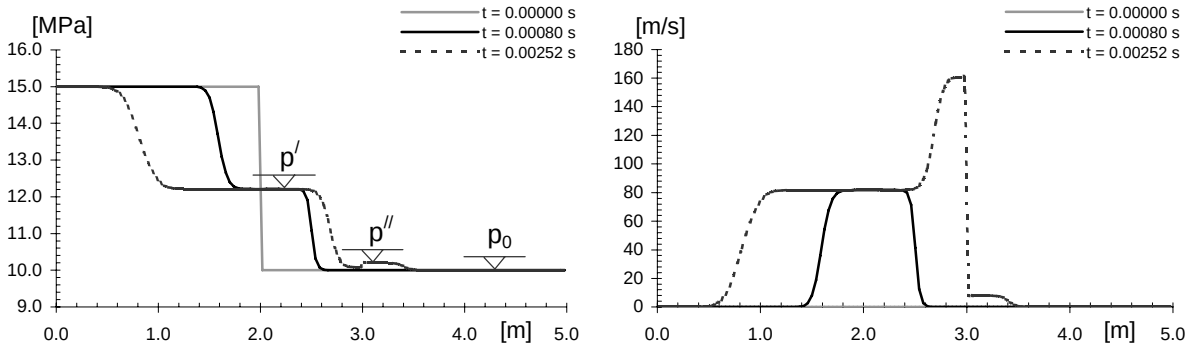

Figure 12: Pressure and velocity profiles at different time.

7.3 Model of flow through the branch

A branch model was developed for the WAHA code to connect three pipes in a single point (Fig. 13). A junction of more than three pipes in a single point is not allowed in the WAHA code. A branch does not have a volume; it is merely a point that connects three pipes. Treatment of the branch connection is discussed by Martin and Wiggert (1996), and by Wylie and Streeter in the sections 3-5 of their book (1978). A slightly modified version of their approach is used in the WAHA code. In the branch model a "dominant" pipe is defined first, as a pipe with the largest mass flow rate:

$$\phi_{main} = \max\left(\phi_1, \phi_2, \phi_3\right), \tag{30}$$

where ϕ_i are mass flows in the connected pipes. The state in the other two connected pipes is averaged. In the case, when the main pipe has index $i = 1$, the averaged state is

$$p_{av} = \frac{p_2 A_2 + p_3 A_3}{A_2 + A_3} \quad \alpha_{av} = \frac{\alpha_2 A_2 + \alpha_3 A_3}{A_2 + A_3} \tag{31}$$

$$v_{k,av} = \frac{\alpha_{k,2}\rho_{k,2}v_{k,2}A_2 + \alpha_{k,3}\rho_{k,3}v_{k,3}A_3}{\alpha_{k,2}\rho_{k,2}A_2 + \alpha_{k,3}\rho_{k,3}A_3} \tag{32}$$

$$u_{k,av} = \frac{\alpha_{k,2}\rho_{k,2}u_{k,2}A_2 + \alpha_{k,3}\rho_{k,3}u_{k,3}A_3}{\alpha_{k,2}\rho_{k,2}A_2 + \alpha_{k,3}\rho_{k,3}A_3} \qquad k = f, g$$

The boundary values in the pipes are then calculated in the same was as in the abrupt area change model with $\vec{\psi}_1 \leftarrow \vec{\psi}_{main}$, $\vec{\psi}_2 \leftarrow \vec{\psi}_{av}$ and $A_2 \leftarrow (A_2 + A_3)$.

After the abrupt area change calculation is finished the boundary values in the dominant pipe 1 are already prescribed, while the values of the averaged pipe are taken as boundary values of the pipes 2 and 3, except the phasic velocities, which are not taken as the velocity of the averaged pipe, but are extrapolated from the pipes 2 and 3.

Two-phase shock tube with a branch. This case shows behaviour of the pressure pulse through the branch filled with pure liquid. A sketch of the modelled branch is shown in Fig. 13.

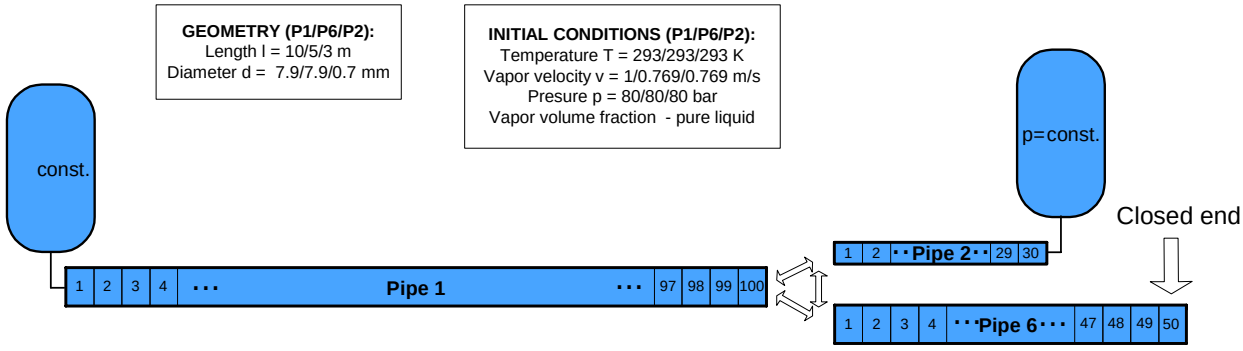

Figure 13: Geometry and initial conditions of the single-phase branch model.

The left pipe is 10 m long and its left end is connected to a large water tank modelled as a constant pressure boundary condition. The upper pipe is 3 m and the right pipe is 5 m long. The left and the right pipe have the same cross-section A = 0.1 m^2, while the upper pipe has the cross-section $A_2 = 0.03\ m^2$. Initially, the following stationary state is applied: $\rho_1 = \rho_2 = \rho_6 = 1001.9\ kg/m^3$, $v_1 = 1$ m/s, $v_2 = v_6 = 0.769$ m/s and $p_1 = p_2 = p_6 = 80$ bar. The flow direction is from the tank on the left, through the pipe 1 into the pipes 2 and 3. At the time $t = 0$, the right end of the pipe 6 is closed and the pressure pulse expands through the piping system. Figure 14 shows the time history of the pressure in the points 1, 2 and 3, which are located 1.05 m from the end of the pipe 1

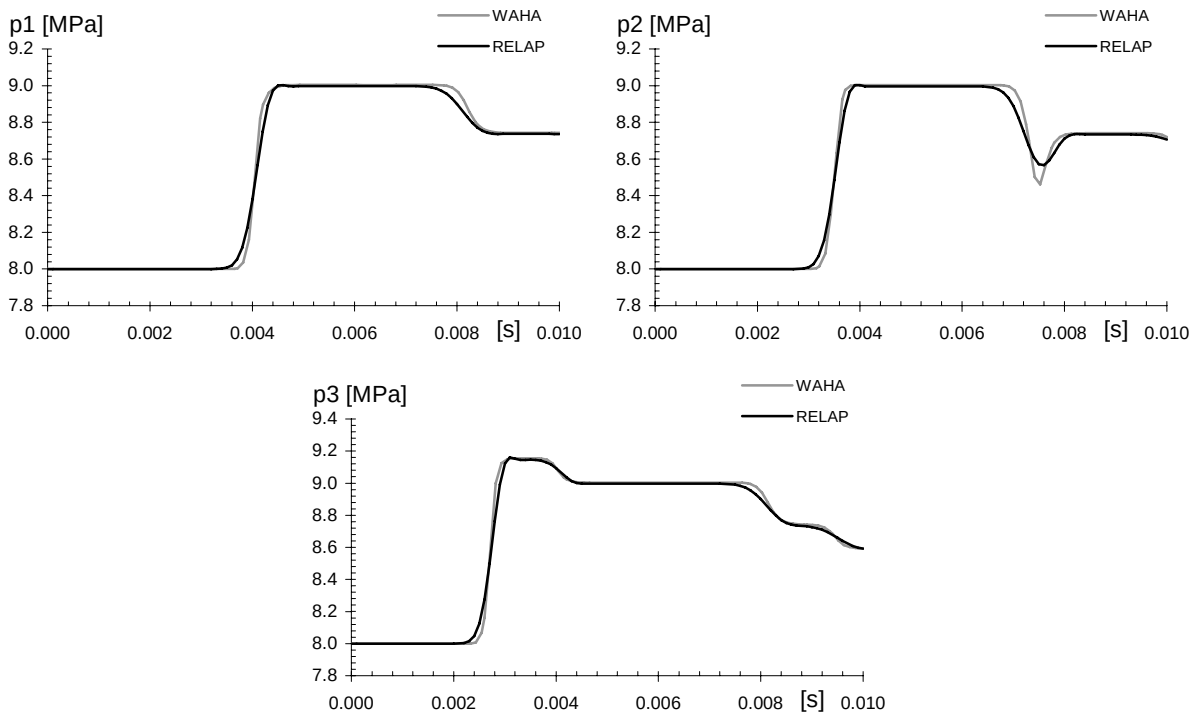

Figure 14: Comparison of the WAHA and RELAP5 pressure history in the points 1, 2 and 3 - single-phase liquid case.

(point p1), 0.15 m from the beginning of the pipe 6 (point p2), and 0.95 m from the beginning ofthe pipe 2 (point p3). The WAHA code results are compared with RELAP5/MOD3.3 code simulation. The only differences are due to the less diffusive numerical scheme in the WAHA code.

The abrupt area change model and the branch model were tested and verified for the single-phase liquid and gas flows, but have not been thoroughly tested in the various two-phase situations. Thus, the model is to be used with caution in two-phase systems, especially in the horizontal two-phase flows where stratification might appear. The reduced CFL number is recommended with values ~0.5, if problems with the abrupt area change model appear.

The current abrupt area change and branch models do not contain generation or loss of momentum and energy. These models, especially momentum losses, can be included into the abrupt area change and branch models as additional wall friction coefficients in the nodes near the connection to obtain more realistic flow behaviour.

8. Conclusions

The present work describes the numerical scheme used to solve the 1D six-equation two-fluid model in the WAHA code. Rather "standard" numerical scheme was used for the hyperbolic part of the equations. New approach is applied for the non-relaxation terms, which are integrated with a similar scheme as the hyperbolic part of the equations. Such approach preserves steady-state solutions (e.g. steady flow in ducts of variable cross-section, or steady-state flows in vertical pipes under the influence of gravity). Operator splitting is used only for the relaxation terms due to their stiffness. Moreover, operator splitting of the stiff relaxation sources introduces numerical error similar to numerical diffusion.

The results obtained with the WAHA code are available in the WAHA3 (current code version) code manual on internet (see Tiselj et. al. 2004). They include different single-phase gas and liquid tests. Some of these results are compared with results of the numerical scheme with conservative form of the Euler equations.

Further modifications of the WAHA code, such as an implicit integration scheme for the relaxation source terms, and more detailed treatment of the single to two-phase flow transition , could be implemented. Other changes are mainly related to the possible new physical models in the code, like fluid-structure interaction modelling and introduction of an additional equation that would trace the amount of the non-condensible gas in the vapor phase.

Acknowledgements
Authors were supported by the Ministry of Education, Science and Sport of Republic of Slovenia and within the WAHALoads project of the 5th Framework Programme of European Union - Euratom.

References

1. Abgrall, R., 1996, How to prevent pressure oscillations in multicomponent flow calculations: a quasi conservativ approach, *Journal of Computational Physics* **125**, 150-160.
2. Anderson, J.D., 1995, Computational Fluid Dynamics, McGraw-Hill, New York.
3. Bereux, F., 1996, Zero-relaxation limit versus operator splitting for two-phase fluid flow computations, *Computer Methods in Applied Mechanics and Engineering* **133**, 93-124.
4. Bestion, D., 1990, "The Physical Closure Laws in the CATHARE Code", *Nuclear Engineering and Design* **124**, No. 3.
5. Burman, E., Sainsaulieu, L., 1995, Numerical analysis of two operator splitting methods for an hyperbolic system of conservation laws with stiff relaxation terms, *Computer Methods in Applied Mechanics and Engineering* **128**, pp. 291-314.
6. Carlson, K.E., Riemke, R.A., Rouhani, S.Z., Shumway, R.W., Weaver, W.L., 1990, *RELAP5/MOD3 Code Manual, Vol. 1-7*, **NUREG/CR-5535**, EG&G Idaho, Idaho Falls.
7. Edwards, A.R., O'Brien, F.P., 1970, Studies of phenomena connected with the depressurization of water reactors, *Journal of the British Nuclear Society* **9**, 125-135.
8. Evje, S., Fjelde, K.K., 2002, Hybrid Flux-Splitting Schemes for a Two-Phase Flow Model, *Journal of Computational Physics*, **175(2)**, 674-701.
9. Evje, S., Flatten, T., 2003, Hybrid flux-splitting schemes for a common two-fluid model, *Journal of Computational Physics* **19**2 (1), 175-210.
10. Faucher, E., Herard, J. M., Barret, M., Toulemonde, C., 2000. Computation of flashing flows in variable cross-section ducts, *International Journal of Computational Fluid Dynamics* **13**, 365-391.
11. Gale, J., Tiselj, I., Horvat, A., Parzer, I., 2006, The two-fluid model of the WAHA code for simulations of the water hammer transients, submitted to *Multiphase Science and Technology*.
12. Gallouet, T., Massela, J.M., 1996, A rough Godunov scheme, *C.R.A.S. Paris*, **323**, 77-84.
13. Ghidaglia, J. M., Kumbaro, A., Le Coq, G., 2001. On the solution of the two fluid models via a cell centered finite volume method, *Eur. J. Mech. B - Fluids* **20**, 841-867.
14. Glaister, P., 1985, *Flux difference splitting techniques for the Euler equations in non-cartesian geometry*, Numerical analysis report 8/85, University of Reading.
15. Guinot, V., 2001. Numerical simulation of two-phase flow in pipes using Godunov method, *Int. J. Num. Methods Eng.* **50**, 1169-1189.

16. Hirsch, C., 1988, *Numerical computation of internal and external flow*, Vol. 1-2, John Wiley & Sons.
17. Karni, S., 1996. Hybrid Multifluid Algorithms, *SIAM J. Scientific Computing* **17** (5), 1019-1039.
18. LeVeque, R.J., 1992, Numerical Methods for Conservation Laws, *Lectures in Mathematics, ETH, Zurich*.
19. Martin, C.S., D. Wiggert, D., 1996, *Waterhammer and fluid structure interaction in piping system*, Materials from ASME Professional Development Programs.
20. Paillere, H., Corre, C., Garcia Cascales, J. R., 2003. On the extension of the AUSM+ scheme to compressible two-fluid models, *Computers and fluids*, **32** (6), 1497-1530.
21. Pember, R.B., 1993, Numerical Methods for Hyperbolic Conservation Laws with Stiff Relaxation I. Spurious Solutions", *SIAM J. Appl. Math.* **53**, No. 5, 1293.
22. Ransom, V.H., 1987, Numerical benchmark tests, *Multiphase Science and Technology 3*, Hemisphere, Washington DC.
23. Roe, P.L., 1981, Approximate Riemann solvers, parameter vectors and difference schemes, *Journal of Computational Physics* **43**, 357-372.
24. Saurel, R., Abgrall, R., 1999, A Multiphase Godunov method for compressible multifluid and multiphase flows, *Journal of Computational Physics* **150**, 425-467.
25. Seynhaeve, J.M., Water properties package, Catholic University of Louvain, (1992), built with IAPS from Lestler, Gallaher and Kell, Mc Graw-Hill 1984 - NBS reference.
26. Sod, G.A., 1978, A Survey of several finite difference methods for systems of nonlinear hyperbolic conservation laws, *Journal of Computational Physics*, **27**, 1-31.
27. Spore, J. W. Weaver, W.L., Shumway, R.W., Giles, M.M., Phillips, R.E., Mohr, C.M., Singer, G.L., Aguilar, F., Fischer, S.R., 1981, "TRAC-BD1 - Transient Reactor Analysis Code for Boiling Water Systems", Transient Two-Phase Flow, Proceedings of the Third CSNI Specialist Meeting, 533-550, Pasadena, California.
28. Tiselj, I., Petelin, S., 1997, Modelling of two-phase flow with second-order accurate scheme, *Journal of Computational Physics* **136** (2) 503-521.
29. Tiselj, I., Petelin, S., 1998, First and Second-order accurate schemes for two-fluid models, *Journal of Fluids Engineering - ASME* **120** (2), 363-368.
30. Tiselj, I., Horvat, A., 2002, Accuracy of the operator splitting technique for two-phase flow with stiff source terms, *Proceedings of ASME Joint U.S.-European Fluids Engineering Conference*, Montreal.
31. Tiselj, I., Gale, J., Horvat, A., Parzer, I., 2003, Characteristic and propagation velocities of the two-fluid models, *Proceedings of the 10th International Topical Meeting on Nuclear Reactor Thermal Hydraulics (NURETH-10)*, Seoul, Korea, October 5-9.
32. Tiselj, I., Černe, G., Horvat, A., Gale, J., Parzer, I., Giot, M., Seynhaeve, J. M., Kucienska, B., Lemonnier, H., 2004, WAHA3 code manual, WAHALoads project deliverable D10, Download: http:\\www2.ijs.si\~r4www\WAHA3_manual.pdf
33. Toumi, I., Kumbaro, A., 1996, An Approximate Linearized Riemann Solver for a Two-Fluid Model", *Journal of Computational Physics*, **124**, 286.
34. Wylie, E.B., Streeter, V. L., 1978, Fluid Transients, McGraw-Hill.